Author(s): Magron, C.; Alfaurt, Ph.; Blank, B.; Daudin, L.; Eronen, Tommi; Gerbaux, M.; Giovinazzo, J.; Gorelov, Dmitry; Grévy, S.; Guérin, H.; Hakala, Jani; Kolhinen, Veli; Koponen, Jukka; Nieto, T. Kurtukian; Moore, Iain; Penttilä, Heikki; Pohjalainen, Ilkka; Reinikainen, Juuso; Reponen, Mikael; Rinta-Antila, Sami; Roche, M.; Roubin, A. de; Smirnova, N.; Thomas, B.; Voss, Annika; Xayavong, L.

Title: Precise measurements of half-lives and branching ratios for the ββ mirror transitions in the decay of 23Mg and 27Si

Year: 2017

Version:

Please cite the original version:

Magron, C., Alfaurt, P., Blank, B., Daudin, L., Eronen, T., Gerbaux, M., Giovinazzo, J., Gorelov, D., Grévy, S., Guérin, H., Hakala, J., Kolhinen, V., Koponen, J., Nieto, T. K., Moore, I., Penttilä, H., Pohjalainen, I., Reinikainen, J., Reponen, M., . . . Xayavong, L. (2017). Precise measurements of half-lives and branching ratios for the ββ mirror transitions in the decay of 23Mg and 27Si. European Physical Journal A, 53(4), Article 77. https://doi.org/10.1140/epja/i2017-12271-0

EPJ manuscript No.
(will be inserted by the editor)

Precise measurements of half-lives and branching ratios for the β mirror transitions in the decay of ^{23}Mg and ^{27}Si

C. Magron[1], Ph. Alfaurt[1], B. Blank[1], L. Daudin[1], T. Eronen[2], M. Gerbaux[1], J. Giovinazzo[1], D. Gorelov[2], M. Grévy[1], H. Guérin[1], J. Hakala[2], V.S. Kolhinen[2], J. Koponen[2], T. Kurtukian Nieto[1], I.D. Moore[2], H. Penttilä[2], I. Pohjalainen[2], J. Reinikainen[2], M. Reponen[2], S. Rinta-Antila[2], M. Roche[1], A. de Roubin[1,3], N. Smirnova[1], B. Thomas[1], A. Voss[2], and L. Xayavong[1]

[1] Centre d'Etudes Nucléaires de Bordeaux Gradignan, UMR 5797 CNRS/IN2P3 - Université de Bordeaux, 19 Chemin du Solarium, CS 10120, F-33175 Gradignan Cedex, France
[2] University of Jyvaskyla, Department of Physics, P.O.Box 35, FI-40014 University of Jyvaskyla, Finland
[3] Max-Planck-Institut für Kernphysik, P.O Box 103980, D-69029 Heidelberg, Germany

the date of receipt and acceptance should be inserted later

Abstract Half-lives and branching ratios for the two mirror β decays of ^{23}Mg and ^{27}Si have been measured at the University of Jyväskylä with the IGISOL facility. The results obtained, $T_{1/2} = 11.303(3)$ s and $T_{1/2} = 4.112(2)$ s for the half-lives of ^{23}Mg and ^{27}Si, respectively, are 7 and 8 times more precise than the averages of previous measurements. The values obtained for the super-allowed branching ratios of ^{23}Mg and ^{27}Si are $B.R. = 92.18(8)\%$ and $B.R. = 99.74(2)\%$, respectively. The result for ^{23}Mg is three times more precise than the average of the previous measurements, while for ^{27}Si the precision has not been improved, the average of the previous measurements being already very precise. Isospin-symmetry breaking corrections have been calculated for the two nuclei to determine the corrected $\mathcal{F}t$ value.

PACS. XX.XX.XX No PACS code given

1 Introduction

The nuclear β decay is an important weak-interaction process to test the Standard Model of particle physics and underlying symmetries. In particular, the transitions involving the vector component of the weak current (Fermi transitions) allow us to verify the conserved vector current (CVC) hypothesis and, if it holds, the unitarity of the Cabibbo-Kobayashi-Maskawa (CKM) quark-mixing matrix. Four kinds of weak decays are used to perform these tests: i) pion decay, ii) super-allowed $0^+ \rightarrow 0^+$ Fermi transitions, iii) free neutron decay, and iv) mirror nuclear β transitions. Super-allowed $0^+ \rightarrow 0^+$ transitions, which are of pure Fermi type, provide the most accurate tests, whereas the results from pion, free neutron and mirror decays are one order of magnitude less precise.

The CVC hypothesis implies that the vector part of the weak interaction is not impacted by the nuclear medium that is to say the vector coupling constant, G_V, is unique for all weak processes. To verify this hypothesis the corrected $\mathcal{F}t$ value must be determined. For super-allowed $0^+ \rightarrow 0^+$ transitions, the expression is [1]:

$$\mathcal{F}t = f_V t \left(1 + \delta_R^{'}\right)(1 + \delta_{NS} - \delta_C) = \frac{K}{G_V^2 \langle M_F^0 \rangle^2 \left(1 + \Delta_R^V\right)},$$

where f_V is the statistical rate function for the vector part of the interaction depending on Q_{EC}, the energy of the transition. t is the partial half-life and is equal to $T_{1/2}(1 + P_{EC})/B.R.$, $T_{1/2}$ being the half-life of the parent nucleus, $B.R.$ the branching ratio of interest and P_{EC} the probability of electron capture (EC) [1]. $\delta_R^{'}$ and Δ_R^V are the transition-dependent and transition-independent parts of the radiative corrections, respectively. δ_{NS} is a nuclear structure dependent radiative correction, and δ_C is the isospin-symmetry breaking correction. Theses corrections are determined theoretically by models (see Ref. [1]). K is a constant and $\langle M_F^0 \rangle$ is the Fermi matrix element which is equal to $\sqrt{T(T+1) - T_{zi}T_{zf}}$, where T is the isospin of the decaying nucleus and T_{zi} and T_{zf} are the isospin projection for the initial and final states, respectively.

According to the CVC hypothesis, this "corrected $\mathcal{F}t$" value must be constant for all super-allowed $0^+ \rightarrow 0^+$ transitions of a given isospin. Currently, 14 super-allowed Fermi transitions between ^{10}C and ^{74}Rb are used to determine a mean $\mathcal{F}t$ value, resulting in $\overline{\mathcal{F}t} = 3072.27(62)$ s (0.02% precision) [1].

Mirror β decays are mixed Fermi and Gamow-Teller transitions for which the $\mathcal{F}t$ value is no longer a constant. Taking this mixing into account, one can introduce $\mathcal{F}t_0$ as follows [2]:

$$\mathcal{F}t_0 = f_V t \left(1 + \delta_R^{'}\right)(1 + \delta_{NS} - \delta_C)\left(1 + \frac{f_A}{f_V}\rho^2\right)$$

$$= \frac{K}{G_V^2 \langle M_F^{T=1/2} \rangle^2 \left(1 + \Delta_R^V\right)}$$

where f_A is the statistical rate function for the axial-vector part of the interaction, and $\rho \approx \frac{G_A \langle M_{GT}^{T=1/2} \rangle}{G_V \langle M_F^{T=1/2} \rangle}$ is the mixing ratio of Fermi and Gamow-Teller transitions [2]. G_A and $\langle M_{GT} \rangle$ are the axial-vector coupling constant and the Gamow-Teller matrix element, respectively. The theoretical corrections determined using the same models as for pure Fermi transitions are compiled in [3].

According to the CVC hypothesis, $\mathcal{F}t_0$ is a constant for mirror β decays. These transitions were recently "rediscovered" for this test [2]. However, only for five mirror transitions (from ^{19}Ne to ^{37}K) all parameters are measured and can be used to determine a mean $\mathcal{F}t_0$ value: $\overline{\mathcal{F}t_0} = 6173(22)$ s (0.4% precision).

Beta plus decay acts at the elementary level by a transformation of an *up* quark into a *down* quark and gives access to the V_{ud} coefficient of the CKM matrix. It is determined from the following expression:

$$V_{ud} = \frac{G_V}{G_\mu},$$

where G_μ is the coupling constant of the purely leptonic muon decay [4].

The CKM matrix describes the mixing of the mass eigenstates of the three generations of quarks into eigenstates of the electroweak interaction. In a three generation model, this matrix has to be unitary, with e.g. the first row yielding

$$|V_{ud}|^2 + |V_{us}|^2 + |V_{ub}|^2 = 1.$$

In the sum of the first row, V_{ud} is the dominant term. It has been determined for the four weak decays cited above, and the different values are listed in Table 1. Super-allowed Fermi transitions provide today the most accurate value, but improvements on mirror decays are achievable.

To use mirror transitions to verify the CVC hypothesis, to determine the V_{ud} matrix element, and to test the unitarity of the CKM matrix, four experimental quantities have to be measured: the decay Q value, the half-life of the decaying nucleus, the branching ratio of the super-allowed decay branch, and the Gamow-Teller-to-Fermi mixing ratio. For many super-allowed $0^+ \rightarrow 0^+$ transitions, the experimental quantities are known with precisions of the order of 10^{-3} or better. Therefore, for mirror transitions to be competitive with $0^+ \rightarrow 0^+$ transitions, similar precisions are also required.

This paper is dedicated to the mirror decays of ^{23}Mg and ^{27}Si. We will focus on measuring very precisely their half-lives and branching ratios. Prior to the present work, the half-lives of ^{23}Mg and ^{27}Si were known with precisions of 0.27% and 0.36%, respectively, and the branching ratio of ^{23}Mg with a precision of 0.26%. Only the branching ratio of ^{27}Si had a very high precision of 0.02%. The first section of the present paper is dedicated to the experimental procedure, followed by the data analysis. Once the experimental results are obtained, we will discuss these results and place them into the international context of weak interaction studies.

Table 1. Values of V_{ud} for the four weak decays cited in the text. The values are from [4] for pion decay, from [7] for the free neutron decay, from [8] for mirror decays and from [1] for super-allowed $0^+ \rightarrow 0^+$ decays.

decays	V_{ud}	precision (%)
pion	0.9749(26)	0.27
free neutron	0.97520(140)	0.14
mirror	0.97190(170)	0.17
super-allowed	0.97417(21)	0.02

2 Experimental procedure

The experiment took place in late 2013 at the University of Jyväskylä with the IGISOL facility [5,6]. The K130 cyclotron produced a proton beam with an energy of 15 MeV (30 MeV for some runs at the beginning of the experiment). The targets were ^{23}Na and ^{27}Al for ^{23}Mg and ^{27}Si, respectively, produced by means of (p,n) reactions. After mass separation ($\frac{M}{\Delta M} = 500$), beams of ^{23}Mg or ^{27}Si, contaminated only by stable ^{23}Na and ^{27}Al, respectively, were transported to the yield station.

The nuclei ^{23}Mg and ^{27}Si were deposited on a mylar tape (50 μm thickness and 1.25 cm width). The tape moved the sample from the collection point to the measurement point (about 12 cm) between a plastic scintillator for the detection of β particles and a germanium detector for γ rays (see Figure 1). The plastic scintillator was read out by two photomultipliers (PMs). The coincidence signal of these PMs was used to count the β^+

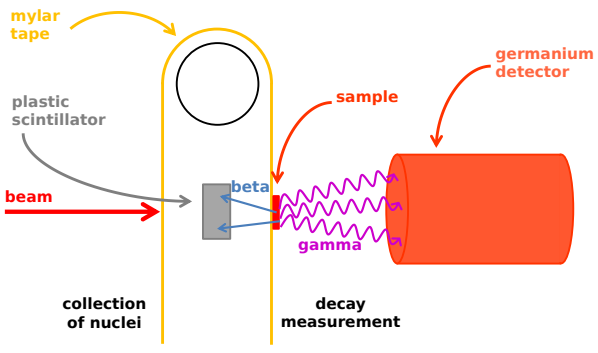

Figure 1. The experimental set-up consisted of a tape for collection and transport of the radioactive samples, a plastic scintillator to detect β particles, and a germanium detector for γ rays. The sample transport was about 12 cm. The distance between the sample once transported to the measurement position and the entrance window of the germanium detector was 15 cm. Figure not to scale.

particles needed to determine the half-lives and to trigger the data acquisition for the branching ratio measurement. The branching ratios were determined by measuring the absolute intensities of the γ rays (440 keV for ^{23}Mg and 2210 keV for ^{27}Si) detected by a germanium detector precisely calibrated in efficiency (order of 10^{-3} [9]). In the present work, we used an efficiency of 0.4053(23)% for the 440 keV γ-ray energy and of 0.124(11)% for the 2210 keV line. These values were determined by a simulation of the decays of ^{23}Mg and ^{27}Si for the germanium detector in the environment of the experiment. The uncertainties of the efficiencies are large as the branching ratios are small and thus the statistics is low in the simulations. However, in both cases this detection efficiency is not the limiting factor for the final precision of the branching ratio.

The experiment consisted in cycles made up of different phases. The first phase was a background measurement before the nuclei of interest were accumulated on the tape. After the collection the tape was moved to position the sample between the plastic scintillator and the germanium detector. The decays were measured for at least ten half-lives. Finally, the tape was moved again to remove the remaining activity. The durations of the different phases are listed in Table 2. The longer decay phases were dedicated to the half-life measurements, the shorter to the branching ratio determination.

For ^{23}Mg, two series of measurements have been done, one with a long decay time optimised for the half-life measurement and one with a short decay time optimised for the branching-ratio measurement (see Table 2). For ^{27}Si, three measurement series were dedicated to half-life measurements, the first set being performed with an energy of the proton beam of 30 MeV, whereas all other measurements were performed with an energy of 15 MeV. For sets 2 and 3, we increased the measurement time for the decay part and the background to achieve better precision. This was possible, as it became clear during the experiment that a statistical precision of 0.1% or below could be reached. No specific measurement has been carried out for the determination of the branching ratio. This choice was made because this parameter is already known very precisely for ^{27}Si.

To register the experimental data, we used three independent data acquisition (DAQ) systems. The first two, DAQ1 and DAQ2, were simple scaler-type DAQs that only registered the time of an event. These scalers were read out every 10 ms and their values stored on disk. These two DAQs were thus used only for the half-life determination with fixed dead-times of 2 μs and 8 μs, respectively.

DAQ3 was of listmode type. It registered the time of an event as well as the energy signal of the germanium detector and of the PMs and was run with a fixed dead time of 200 μs. In addition, the real dead-time was measured on an event-by-event basis. This DAQ was used to determine the half-lives and the branching ratios.

For the first part of the experiment, runs 1-12 for ^{23}Mg as well as runs 1-21 for ^{27}Si, only DAQ3 worked properly and could be used to determine the half-life. For the other runs, all DAQs were operational.

Table 2. Duration of the different phases for the two nuclei studied. Regarding the nucleus ^{23}Mg, two data sets were recorded, the first one was optimised for the half-life measurement and the second for the branching ratio measurement. For ^{27}Si, three sets were recorded, all of them dedicated to the determination of the half-life. See text for more details.

^{23}Mg	first set	second set
background	5.0	5.0
accumulation	30.0	26.0
tape move	0.9	0.9
decays	150.0	26.0
tape move	4.1	4.1

^{27}Si	first set	second set	third set
background	0.5	2.0	5.0
accumulation	12.0	12.0	12.0
tape move	0.9	0.9	0.9
decays	42.0	84.0	84.0
tape move	4.1	4.1	4.1

In total, 1.74×10^7 decays have been recorded for the nucleus ^{23}Mg, distributed over 579 cycles summed into 28 runs. For ^{27}Si, 2.63×10^7 decays have been measured in 2878 cycles, summed into 44 runs.

3 Data analysis

3.1 Half-life

The first step in the analysis procedure is the dead-time correction. DAQ1 and DAQ2 provide only time distributions of the β triggers. The decay-time histograms have to be corrected bin by bin for the fixed dead times of 2 μs and 8 μs, respectively. This correction, c, is calculated for each bin with the following equation:

$$c = \frac{1}{1 - \frac{N \times DT}{T_{bin}}} \quad (1)$$

with N the number of events in a given bin before correction, DT the fixed dead time, and T_{bin} the bin width ($T_{bin} = 0.04$ s for ^{23}Mg, $T_{bin} = 0.025$ s for ^{27}Si).

DAQ3, the list-mode data acquisition, was more difficult to correct. In fact, because of the large amount of information recorded for each event, the DAQ buffer where the event information is stored temporarily was full several times per cycle, and the data transfer to the disk took sometimes longer than the 200 μs of fixed minimum dead time set for the acquisition, the intrinsic dead time of the data acquisition prolonging thus the effective dead time. Therefore, the simple dead-time correction described above could not be applied. The dead time was thus measured on an event-by-event basis, via a 1 MHz clock enabled when the DAQ was "dead". The duration of each event equivalent to the dead-time of the DAQ was stored

event-by-event. This information together with the number of events observed per time interval allowed the dead-time correction to be performed for each event.

Once corrected, the decay phase of each cycle was fitted with an exponential function plus a constant background for each cycle. Cycles were accepted only if the normalized χ^2 was smaller than 2, and if the total number of counts in the cycle was larger than 500. This selection led to a rejection of about 10% of the cycles for ^{23}Mg and of about 3% for ^{27}Si, basically exclusively due to a lack of events in the cycles. Cycles with the same experimental conditions were summed up to form runs and each run was then fitted by an exponential function plus a constant to yield the half-life of the nucleus of interest for each run. The weighted average of these values leads to the final half-life with its statistical error.

To estimate possible systematic uncertainties, several parameters of the experiment and of the analysis have been varied to test their influence on the final result. For the analysis parameters, we varied the time interval (beginning and end) of the decay part on which the fit was performed as well as the limit of χ^2 and the minimum number of counts of the cycle selection. For the experimental parameters, possible influences on the final result of the number of nuclei in the decay phase, of the level of background and of the high voltage of the two PMs were tested.

3.2 Branching ratio

Only the data recorded by the list-mode data acquisition (DAQ3) allow the determination of the branching ratios. This DAQ was triggered by the coincident signal of both PMs. A γ-ray spectrum is constructed for every cycle and summed to form the runs.

The branching ratios of interest are the super-allowed transitions between the ground states of ^{23}Mg and ^{23}Na on the one hand and of ^{27}Si and ^{27}Al on the other hand. To determine these branching ratios, we measured the feeding of excited states in both daughter nuclei by detecting the emitted γ rays at 440 keV in the case of ^{23}Mg and 2211 keV for ^{27}Si.

The integrals of the peaks of interest at 440 keV or 2211 keV have been fitted (run-by-run in the case of ^{23}Mg, for the three series of runs for ^{27}Si) by a Gaussian and a background function yielding, together with the number of β particles detected and the germanium detector efficiency, the γ-decay branching ratios. The weighted average of these values results in the final γ-decay branching ratio for the decay of the excited states. This procedure is only correct, if the β-detection efficiency is the same for all transitions. As the plastic detector measures only an energy loss, this assumption is very well fulfilled for the case of ^{23}Mg where the Q value for the decay to the ground-state differs only little from the one to the excited state. In the case of ^{27}Si, this is no longer true, as the Q values between the ground state and the excited state are significantly different. However, the small difference in β-detection efficiency is negligible compared to the precision achieved in the present work.

Finally the feedings of the ground states are determined from the branching ratios measured in this experiment, completed by other contributions given in ref. [10, 11] including electron capture probabilities.

As for the half-life, a search for systematic uncertainties is necessary. We thus varied the background function as well as the fit energy limits to search for systematic uncertainties. Other parameters like the tape - detector distance (controled with a precision of 0.05 mm for a distance of 150 mm, relative uncertainty $7*10^{-4}$ for the distance) or the beam spot (controlled by means of a diaphragm at the entrance of the set-up with a diameter of 10 mm, relative uncertainty of $6*10^{-4}$ for the distance) have a negligible influence as compared to the precision reached in the present experiment. As for the efficiency of the germanium detector, this detector was calibrated in a measurement program lasting several years to produce a detector model which allows the calculation of its efficiency with a model precision of 0.1-0.2% depending on the γ-ray energy. In the present experiment, this precision was not reached (and not needed) due to limitations in the CPU time.

During the analysis of the runs dedicated to the branching ratio measurement for ^{23}Mg, 2% of the cycles have been rejected for the same reasons as for the selection of cycles for the half-life. 3170 cycles remained which formed 52 runs representing 6.01×10^7 decays. In the case of ^{27}Si, no specific measurement for the branching ratio was made. Cycles and runs used to determine the half-life were used to generate the spectra needed to determine the branching ratio.

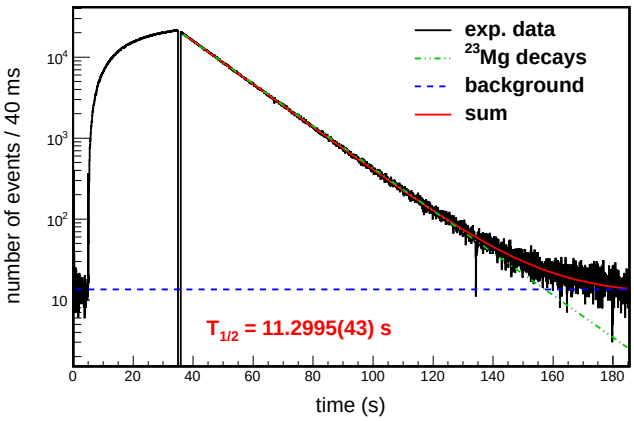

Figure 2. Dead-time corrected time distribution for runs 1 to 12 for DAQ3. The decay phase has been fitted by an exponential function plus a constant (red line), the half-life obtained is indicated. The dotted lines represent the individual contributions from ^{23}Mg and the background. A background measurement, the grow-in phase and the tape transport precede the decay phase.

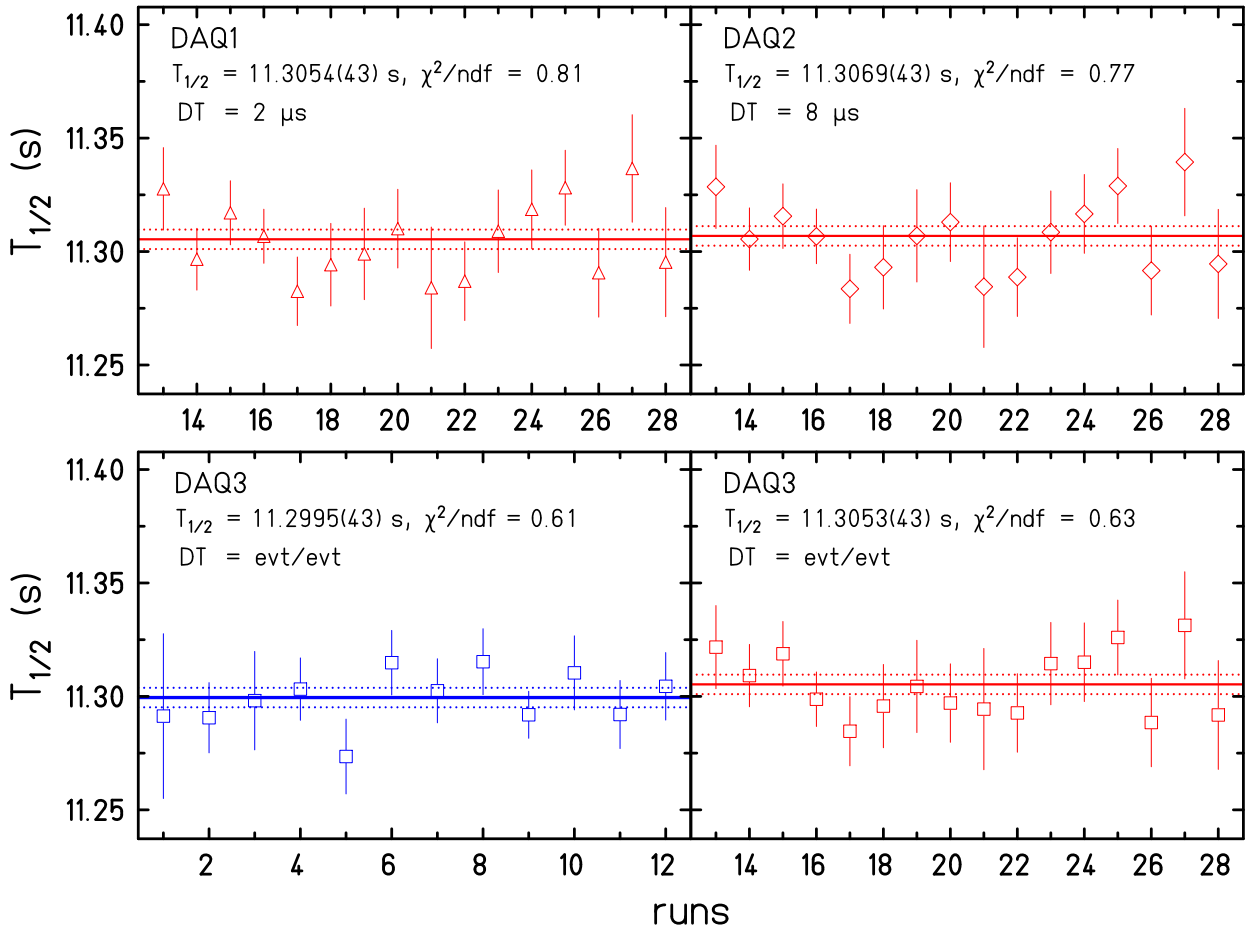

Figure 3. Half-lives of ^{23}Mg as a function of the run number. The top row presents data from DAQ1 and DAQ2, the lower row from DAQ3. On each figure, the average half-life is given together with the fixed dead time. DAQ1 has been corrected for a fixed dead time of 2 μs, DAQ2 for a fixed dead time of 8 μs and DAQ3 for an event-by-event dead time.

To reduce pile-up effects to a negligible level, we kept the counting rate of the germanium detector always well below 1000 counts per second (typically 600-700 counts per second). With a signal shaping time of 2μs for the germanium detector, the pile-up is therefore neglegible.

4 Experimental results

In this section, the results for the half-lives and branching ratios of the nuclei ^{23}Mg and ^{27}Si are presented. First, results with reference parameters are exposed, followed by a study of systematic dependencies before concluding with the final values.

4.1 Half-lives

4.1.1 Result for ^{23}Mg

Results with reference parameters

Figure 2 presents the dead-time corrected decay spectrum of runs 1 to 12 for DAQ3. The half-life values obtained are given in Figure 3. This figure shows the different values determined for the half-life of ^{23}Mg as a function of the run number for the different data acquisitions. As explained above, these data were taken at different moments of the experiment, with DAQ1 and DAQ2 not running correctly at the beginning. On each figure the average half-life determined is specified.

For the first runs of this data set (runs 1-12), the average half-life for DAQ3 is 11.2995(43) s in agreement with the result for the later runs where the same data have

Table 3. The ^{23}Mg half-life values from the literature are compared to our experimental result. The previous weighted average and the one including our value are also given. This last value includes only the most accurate results (see text). All values are in seconds. s is a scaling factor calculated as the square root of χ^2 and applied on the weighted error.

Mihailovic *et al.* [12]	Goss *et al.* [13]	Alburger [14]	Azuelos *et al.*[15]	Azuelos *et al.* [16]	Azuelos *et al.* [17]	This work	Previous average	Present average
12.1(1)	11.41(5)	11.36(4)	11.26(8)	11.327(14)	11.317(11)	11.3027(33)	11.33(3) $s = 3.6$	11.3053(44) $s = 1.4$

been registered with three different DAQs yielding compatible results, the weighted average of these three values being 11.3059(43) s. The error is the average of the three errors because the data are not independent. The final value together with its uncertainty is the weighted average of these two values ($T_{1/2}$ = 11.3027(32) s), the precision being 0.03%. The error is only statistical, so systematic uncertainties have to be evaluated.

Search for systematic dependences

Dead time The time distribution was fitted with the reference parameters by removing one channel (equivalent to 40 ms) at the beginning of the decay part. As shown above, the three DAQs with three different dead times yield results in agreement with each other. Another way to test the influence of the dead time is to cut more and more channels at the beginning. Indeed, it is at the beginning of the decay interval that the number of events is the highest and therefore the dead time correction is the most significant.

Successively, the time cut at the beginning of the decay curve has been increased by steps of 2.5 s or 5 s. The average values of these different cuts for all data sets are presented in Figure 4a). All these cuts lead to an average value staying within the error bars of the reference value.

From these tests, we conclude that no systematic error for the dead time correction needs to be added.

Number of nuclei in the decay phase and in the background The number of nuclei in the decay phase is also a parameter tested for a possible systematic bias. To do so, we assumed that the number of decays for each cycle of a given run is constant. This hypothesis is valid because during a run no parameter has been changed and this is consistent with observation as intensity differences were of the order of 10% or less. Therefore, the only parameter we did not control was the intensity of the beam that was quite constant over a run.

Figure 4b) represents the different half-lives as a function of the number of nuclei in the decay phase. A fit with a constant yields, as expected, the average half-life determined before. As also shown in the figure, a fit with a straight line results in a slope compatible with zero.

We conclude therefore that we have no decay-rate dependence in the determination of the half-life.

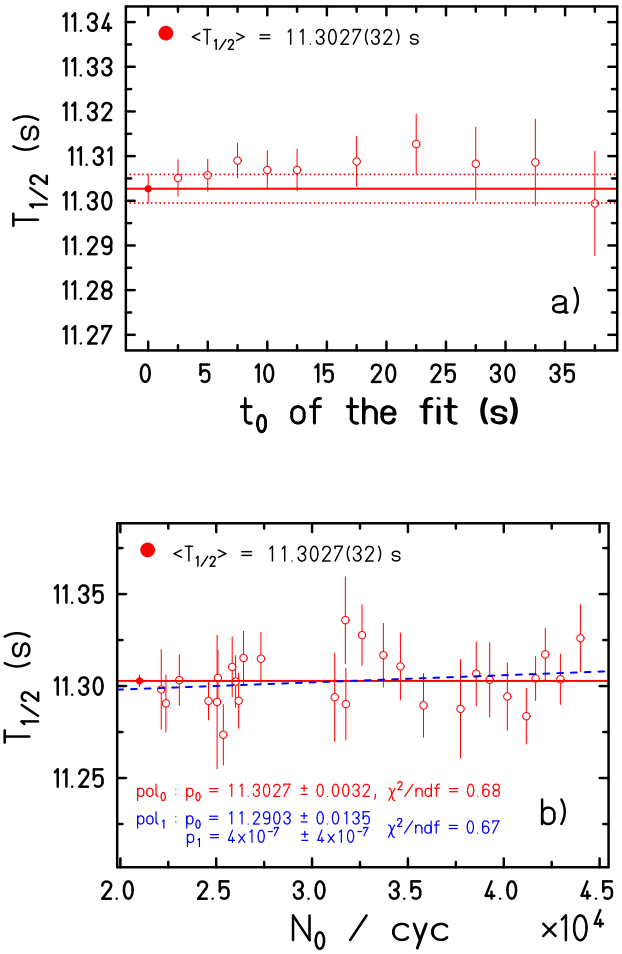

Figure 4. a) Average half-lives of ^{23}Mg for different time cuts. The full red point represents the average half-life quoted in the previous section. The other points are from fits where the start of the fit t_0 was shifted to later times as indicated. b) Half-lives for ^{23}Mg as a function of the number of nuclei, N_0, in the decay phase. The solid red line represents the fit with a constant yielding a half-life of 11.3027(32) s, whereas the dashed blue line is from a fit with a straight line. The parameters of this second fit are also indicated on the figure and show that the slope is compatible with zero (see text for details).

The same test has also been performed for the background level with, again, no evidence of a systematic bias.

Table 4. The ^{27}Si half-life values from the literature are compared to our experimental result. The previous weighted average and the one including our value are also given. All values are in seconds.

Mihailovic *et al.* [12]	Sutton *et al.* [18]	Black *et al.* [19]	Goss *et al.* [13]	Grober *et al.* [20]	Azuelos *et al.* [16]	Genz *et al.* [21]	Barker *et al.* [22]	This work	Previous average	Present average
4.14(3)	4.16(3)	4.19(2)	4.17(1)	4.21(3)	4.109(4)	4.206(8)	4.09(2)	4.1117(20)	4.135(15) $s = 4.7$	4.1181(83) $s = 4.9$

We conclude that there is no systematic dependence of the half-life on the background level.

High voltage of the two photomultipliers Finally, we searched for systematic dependencies as a function of the high voltage of the two PMs (equivalent to different thresholds). These high voltages had been chosen to maximize the triggers for decay events and minimize those from noise of the PMs themselves. To choose the appropriate values, the PMs had been tested before the beginning of the experiment. During the experiment, we varied the two high voltages around the reference values (±100 V). These variations have not shown any systematic modification of the half-life demonstrating that the high voltages do not induce a systematic bias in the resulting half-life.

Conclusion on the search for systematic dependencies None of the parameters tested induced a systematic dependence. However, to be conservative we added the half-difference between the two extreme values of the half-life determined with the three different DAQs, i.e. 0.8 ms as obtained for runs 13 to 28, in quadrature to the statistical error. The final value for the half-life of ^{23}Mg thus determined is 11.3027(33) s, a value with a precision of 0.03%.

Final value for the half-life of ^{23}Mg

Six previous measurements of this half-life are listed by Severijns *et al.* [3] and presented in Table 3. They were used to determine a weighted average which was 11.33(3) s (0.3% precision) before the present work, including a scaling factor for their large scatter (s=3.6) applied to the weighted error. Adding our measurement to the six previous values leads to a new average half-life of 11.306(11) s with a scaling factor of s=3.5. If we employ the method used by Hardy and Towner [1] and remove all values that have an error bar more than 10 times larger than the smallest error bar which eliminates three older results, we obtain an average of 11.3053(44) s (s=1.4), the value we recommend. It has a precision of 0.04% and is about 7 times more precise than the previous average.

4.1.2 Result for ^{27}Si

Results with reference parameters

On Figure 5 the different half-lives determined for ^{27}Si are shown as a function of the run number. For runs 1 to 21, only DAQ3 was functioning correctly. We determined average half-lives of 4.1167(30) s (runs 1-11) and 4.1089(15) s (runs 12-21). For runs 22 to 44, DAQ1, DAQ2 and DAQ3 were functioning and lead to a weighted average of 4.1128(13) s, where the error is the average of the three errors because the data are not independent. The result from all runs 1-44 including a scaling factor of s=1.9 is 4.1117(17) s. The uncertainty is purely statistical. The possible systematic effects are studied in the next paragraph.

Search for systematic dependence

The same parameters as those tested for ^{23}Mg have also been tested for ^{27}Si. We will not give all details here, as the results are the same as for ^{23}Mg. The half-life does not depend on the dead time correction, the number of nuclei in the decay phase, the level of background or the high voltages of the two PMs. As for ^{23}Mg, a systematic dependence can be evaluated as the half-difference between the two extreme values of the half-lives determined with the three DAQs for the same set of data, i.e. 1.1 ms. It has to be added quadratically to the statistical error. The final value of the present experiment for the half-life of ^{27}Si is 4.1117(20) s the precision of which is 0.05%.

Final value for the half-life of ^{27}Si

Eight previous values are quoted in reference [3] and listed in Table 4. The average of these eight values, including a scaling factor ($s = 4.7$), is 4.135(15) s (0.4% precision). As in the case of ^{23}Mg, the large scatter is responsible for this large error bar. Averaging these eight values with our new result yields an average of 4.1181(83) s (0.20% precision, s=4.9) with a significant increase of the precision (almost a factor two).

In the case of ^{27}Si, the elimination of less precise results (a factor of 10 larger error bars as compared to the most precise result) does not improve the average and increases even the scaling factor, a clear indication of the rather large scatter of values given with high precision.

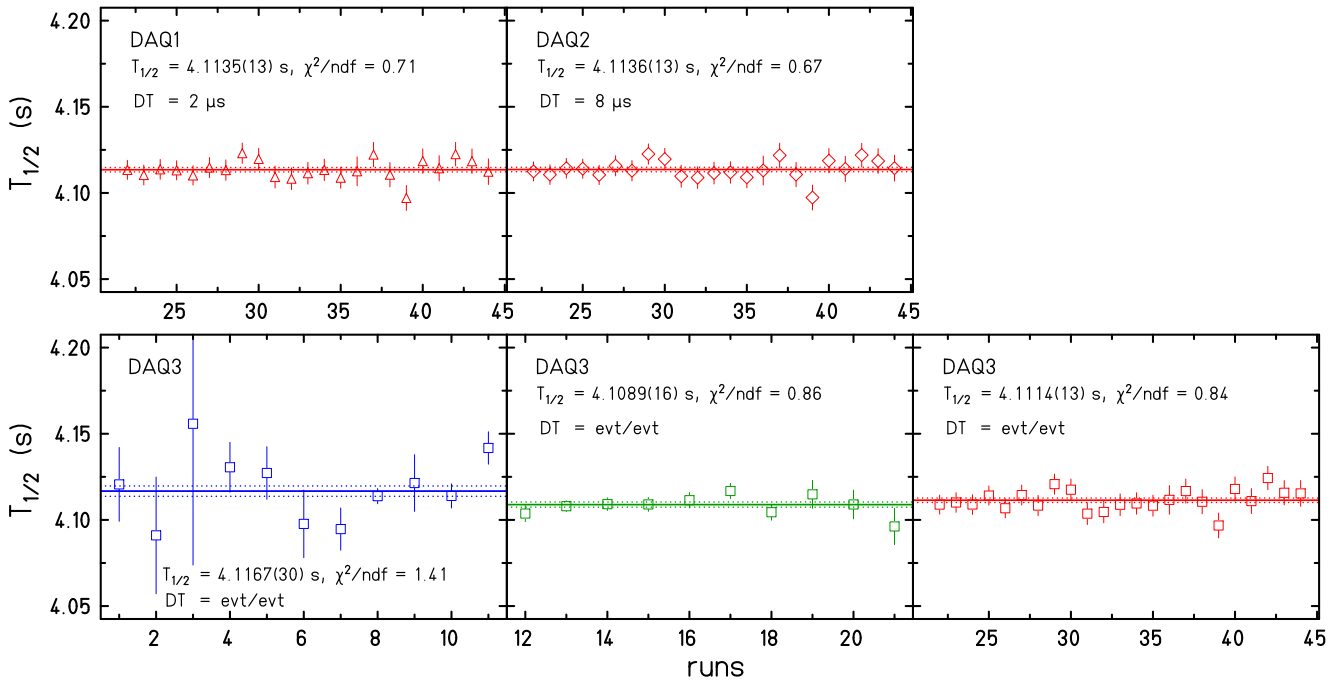

Figure 5. Half-lives of ^{27}Si as a function of the run number. The first row is from DAQ1 and DAQ2, the second from DAQ3. On each figure, the average half-life is given as well as the dead time correction. DAQ1 has been corrected for a fixed dead time of 2 μs, DAQ2 for a fixed dead time of 8 μs and DAQ3 for an event-by-event dead time.

4.2 Branching ratios

4.2.1 Result for ^{23}Mg

Results with reference parameters

Dedicated measurements have been performed to determine the branching ratio of the super-allowed transition of ^{23}Mg. On Figure 6, upper panel, a typical γ-ray spectrum for one run is shown. The lower panel shows the different values of the branching ratio between the ground state of ^{23}Mg and the excited state of ^{23}Na at E=440 keV for all the runs of the experiment dedicated to this measurement. The weighted average is 7.805(79)%. The error is only statistical. To evaluate systematic dependencies, parameters of the analysis have been changed from their reference values. These parameters are: the use of a linear background for the fit of the peak and the fit limits which were ±30 keV around the peak centre for the standard analysis.

Search for systematic dependence

Use of different backgrounds The selection of the background is quite important to determine precisely the number of counts in the peak at 440 keV. In addition to a linear background, we have tested three other background functions for the peak fitting: a quadratic background, a linear step function and a straight line with different slopes left and right of the peak smoothly connected under the peak. The results of these different fits for one run are given in Figure 7. The values shown on the figure for the numbers of counts and the corresponding branching ratios are all consistent with each other. Nevertheless, we can notice that the "linear left-right" background leads to a smaller number of counts and therefore a branching ratio slightly smaller than the others. These results are an example for one run among the 52 runs we registered, but all the runs have been tested and they all behave the same way, with the "linear left-right" background often being different from the three others yielding sometimes larger, sometimes smaller values.

To conclude, the background most likely does not induce a systematic dependence. Nevertheless, we use the half-difference between the reference analysis and the "linear left-right" background (0.016% of absolute uncertainty) as a systematic uncertainty.

Limits of the fit The limits of the fit are particularly tricky to choose because they condition the background definition. They should not be close to the peak, but the peak at 440 keV is close to the Compton edge of the 511 keV annihilation peak (see Figure 6, top panel). Our reference values were ±30 keV around the peak's centre.

Table 5. The β-decay branching-ratio values between the ground state of ^{23}Mg and the excited state at 440 keV of ^{23}Na from the literature are compared to our experimental result. The weighted average of the branching ratio for the 440 keV γ ray has a scaling factor of s=2.1. The ground-state branching ratio also takes into account small branching ratios to the second excited state and the EC contributions (see text for details). All values are in percent.

Talbert *et al.* [23]	Gorodetzky *et al.* [24]	Alburger [14]	Mann *et al.* [25]	Azuelos *et al.* [17]	This work	Average	Ground-state branching ratio
9.1(5)	8.6(3)	9.1(4)	8.1(4)	7.79(15)	7.805(81)	7.91(14)	92.08(14)

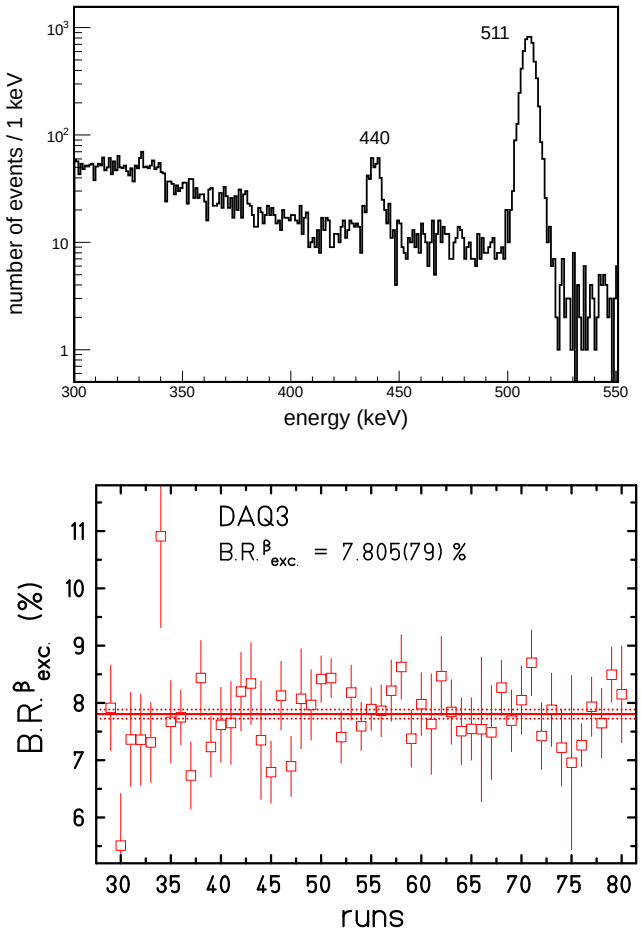

Figure 6. Experimental spectrum (top) in the region of interest for one run and branching ratios determined for the nucleus ^{23}Mg for all runs of the experiment (bottom). The weighted average of these values is given in the figure.

To test the influence of this choice, we used also ranges of ±25 keV. The numbers of counts of the peak for these two limits varied very little (309(25) counts versus 307(25) counts for the example of Figure 7).

This is the case for all the 52 runs dedicated to the measurement of the branching ratio. Therefore, the fit limits do not induce a systematic dependence on the branching ratio.

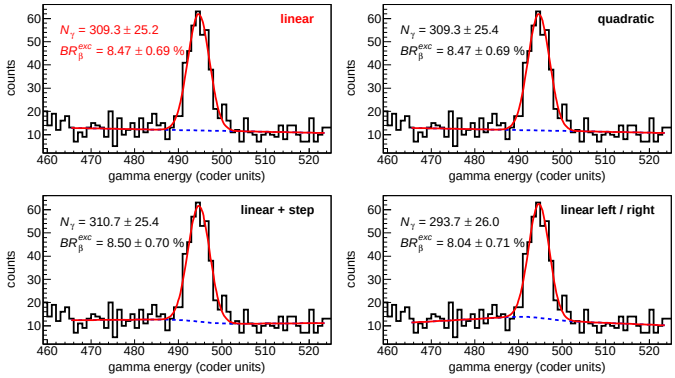

Figure 7. Peak fits with different backgrounds for one run. The background type, the numbers of counts in the peak and the corresponding branching ratios are indicated on each figure. The first figure (top left) presents the fit with the linear background, the reference background, the second (top right) for a quadratic background, followed by the step function background (lower left) and the "linear left-right" background (lower right). All fits have a normalised χ^2 of 1.2.

Final value for the branching ratio of ^{23}Mg

The final value for the γ-decay branching ratio of the 440 keV peak is 7.805% with a statistical uncertainty of 0.079% and a systematic uncertainty of 0.016%. Our final value for the decay of the 440 keV level is thus 7.805(81)%. We note that this is only the part of the branch which is in coincidence with a β particle (≈ 99.9%, see below).

Five other values for this branching ratio have been gathered by Severijns *et al.* [3] and listed in Table 5, their weighted average being 8.13(24)%, this uncertainty takes into account a scaling factor of 2.1. If we add our value, we obtain an average of 7.91(14)% with a scaling factor of 2.1.

The branching ratio we are interested in is the one between the ground states of ^{23}Mg and ^{23}Na. It is obtained by subtracting from 100% the β branching ratio for the 440 keV γ ray in coincidence with β particles as determined here, the branching ratios for the feeding of the excited state at 2390 keV (0.0064(7)% for β feeding, 0.00057(7)% for EC) [10], and the electron capture probabilities for the 440 keV level (0.0103(3)%) given by the same reference. A small correction is still needed because the 440 keV level is also fed in the decay of the 2390 keV level with a branching ratio of 0.0025(3)%. We

obtain therefore $B.R._{gs} = (100-(7.91-0.0025+0.0103+0.0064+0.00057))\%$. Its value is thus 92.08(14)%, with a precision of 0.15%. This ground-state branching ratio includes a small EC contribution of 0.0676(2)% [10]. Compared to the value determined by Severijns *et al.* [3] of 91.78(26)% the precision is improved by almost a factor of 2.

4.2.2 Result for ^{27}Si

Results with reference parameters

No specific measurement has been made to determine the super-allowed branching ratio of ^{27}Si because it is already known very precisely ($\Delta B.R._{gs}/B.R._{gs} = 0.02\%$). We used the three data sets registered for the half-life measurement to determine the branching ratio. As the branching ratio between the ground state of ^{27}Si and the third excited state of ^{27}Al, the strongest branch except for the super-allowed branch, is very weak, a fit could not be performed for each run. All the runs of the three data sets were added separately and a fit was performed for the sum spectra of the three series. The reference parameters were a linear background with fit limits at $\pm$100 keV from the peak centre. The three branching ratios for the 2211 keV peak were 0.179(58)%, 0.188(44)%, and 0.134(41)%. All these values are consistent with each other. The systematic dependences are studied in the next paragraph.

Search for systematic dependence

As for the determination of the branching ratio of ^{23}Mg, different types of backgrounds and different fit limits were tested. The quadratic, linear step, "left-right" backgrounds have been used. The half-difference between the reference background and the linear "left-right" background (which provides the most different results) has been chosen to be the systematic difference, the values obtained are 0.017%, 0.011% and 0.015%. The different fit limits tested were $\pm$50 and $\pm$200 keV. The systematic dependence has been evaluated as the half-difference between the reference limits and those which provide the most different result, the values obtained being 0.006%, 0.009% and 0.005% for the three data sets. Finally, due to the small number of counts in the spectra, the binning has been tested, the reference being 1 keV per channel, we tested 2 keV per channel. The systematic dependence has been evaluated as the difference between the result obtained with these two binnings, the values are 0.013%, 0.002% and 0.007% for the three data sets. These systematic errors have been summed quadratically with the statistical error for each data sets. The results obtained are 0.179(62)%, 0.188(46)% and 0.134(44)%. All these values are consistent with each other, the weighted average being 0.164(28)%.

Final value for the branching ratio of ^{27}Si

Five previous measurements have been gathered by Severijns *et al.* [3] and listed in Table 6, the weighted average of these values being 0.150(10)% (taking into account a scaling factor of 1.7). If averaged with our result, we obtain 0.151(9)% with a scaling factor of 1.5. We note that the value which causes problems is the one from Gorodetzky *et al.* [26] which is the oldest value and given only in a conference paper. It is at about 2.5 σ of the average of the other results. Eliminating this value would yield a slightly higher average value with a scaling factor of 1.1.

The branching ratio of interest is the one between the ground states of ^{27}Si and ^{27}Al which is obtained by subtracting from 100% the present weighted average for the 2212 keV line as well as the other β branching ratios and electron capture probabilities from reference [11]. We obtain $B.R._{gs}$=(100-(0.151+0.046+0.069))% = 99.74(2)% (0.02% precision), with the last two values in the sum being the other β-decay feedings and all EC contributions, respectively.

4.3 Summary of experimental results

All experimental results averaged with literature values are summarised in the decay schemes presented in Figure 8. Half-lives and branching ratios reach now a precision at the few per mil level which satisfies the requirements for weak-interaction studies.

5 Theoretical corrections due to isospin non-conservation

As mentioned in the introduction, several theoretical corrections are needed to deduce the absolute $\mathcal{F}t$ value for super-allowed $0^+ \rightarrow 0^+$ transitions or $\mathcal{F}t_0$ for mirror decays. We will focus here on the isospin-symmetry-breaking correction (δ_c), which is defined as a deviation of the Fermi matrix element squared from its model-independent value:

$$M_F^2 = \langle M_F^0 \rangle^2 \, (1 - \delta_c) \; . \qquad (2)$$

Work is ongoing by different collaborations in order to determine δ_c for the $0^+ \rightarrow 0^+$ decays (see e.g. [1,29]). However, in the case of mirror decays, only two calculations are available: that of Severijns *et al.* [3] within the shell model and that of Satula *et al.* [30] within projected density-functional theory.

In the present work, we propose a new shell-model calculation of the isospin-symmetry-breaking correction for the two nuclei under consideration in an approach similar to that of Towner and Hardy (see [3,31] and references therein) and Ormand and Brown [32]. Within the shell-model formalism, the correction can be separated into two parts: the configuration mixing part (δ_{c1}) and the radial overlap part (δ_{c2}), i.e.

$$\delta_c = \delta_{c1} + \delta_{c2} \, .$$

Table 6. The β-decay branching-ratio values between the ground state of ^{27}Si and the excited state of ^{27}Al at 2212 keV from the literature are compared to our experimental result. The weighted average of this branching ratio and the ground-state to ground-state β-decay branching ratio are also given. All values are in percent.

Gorodetzky *et al.* [26]	Berenyi *et al.* [27]	Détraz *et al.* [28]	Mann *et al.* [25]	Azuelos *et al.* [17]	This work	Average	Super-allowed branching ratio
0.10(2)	0.18(5)	0.15(7)	0.181(14)	0.148(7)	0.164(28)	0.151(9)	99.74(2)

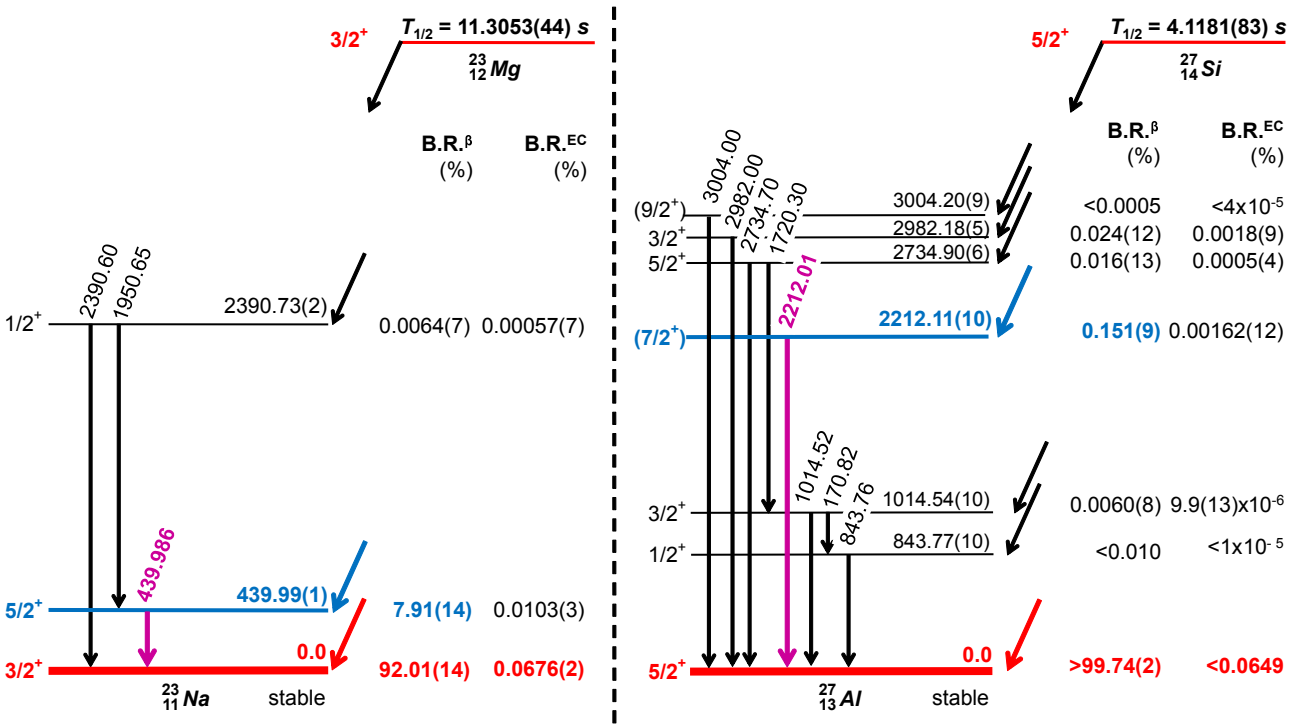

Figure 8. Decay schemes of the two nuclei studied in the present work. The quantities given in the figure are average values from all existing experimental work. In purple, the γ rays observed, in blue the experimentally determined β-decay branching ratios, and in red the ground-state branching ratios.

To get the former, the Fermi matrix element is calculated using shell-model wave functions from an isospin-nonconserving Hamiltonian and harmonic-oscillator radial single-particle wave functions. For the latter, M_F is determined from an isospin-conserving Hamiltonian with, however, realistic spherical Woods-Saxon or Hartree-Fock single-particle wave functions.

We used the NuShellX@MSU [33] code with isospin-conserving *sd*-shell interactions, namely the USD interaction [34] and its more recent versions, USDA and USDB [35]. The isospin-nonconserving Hamiltonians used to calculate δ_{c1} are based on the interactions cited above with the addition of the Coulomb interaction and charge-symmetry breaking and charge-dependence breaking terms as proposed in Ref. [36]. The results obtained from the three different interactions are used to establish the average and the theoretical uncertainty for the correction.

To get the radial-overlap part of the correction (δ_{c2}), we use the single-particle wave functions obtained from a spherical Woods-Saxon potential with parameters (depth V_0 and length parameter r_0) adjusted to experimental data on the charge radius and the proton and neutron separation energies. We go beyond a closure approximation for both, the Fermi matrix element and the charge radius, inserting thus a sum over intermediate states. We have checked that 100 states of each angular momentum is sufficient to get convergence of the results. More details about the calculations can be found in a PhD thesis [37] and a future publication. The three different shell-model interactions produce almost the same results. Since, the error bar on the charge radius is small for the nuclei of interest, the theoretical uncertainty of the correction is very small.

The results of these calculations are given in Tab. 7 in comparison with the values from Severijns *et al.* [3] and Satula *et al.* [30]. One can notice that our correction for ^{23}Mg is smaller than that of Ref. [3] because of a significant difference in the radial-overlap part. At the same time, the value of the correction for ^{27}Si matches that of Ref. [3], although the radial overlap part is bigger which

Table 7. Isospin symmetry breaking corrections determined in the present work in comparison to the values of Severijns *et al. [3]* and Satula *et al. [30]*. See text for details.

isotope	δ_{c1} (%) Severijns 2008 [3]	δ_{c1} (%) present work	δ_{c2} (%) Severijns 2008 [3]	δ_{c2} (%) present work	δ_c (%) Severijns 2008 [3]	δ_c (%) present work	δ_c (%) Satula (2012) [30]
^{23}Mg	0.023(10)	0.015	0.270(20)	0.186	0.293(22)	0.201	0.340
^{27}Si	0.052(30)	0.027	0.260(15)	0.285	0.312(33)	0.312	0.472

is compensated by a smaller value of δ_{c1}. In the presnet paper, we do not give error bars which have to await a complete study of $0^+ \rightarrow 0^+$ and mirror decays over several nuclear shells.

The differences in the δ_{c1} values are due to different parameterizations of charge-dependent terms in the effective interactions used. The difference in δ_{c2} values may partly be due to somewhat different methods of adjustment. For example, Severijns *et al.* may have added some specific surface terms to the WS potential. Besides, we remark that our calculation of the nuclear charge radius involves a complete sum over intermediate states, while Severijns *et al.* used a closure approximation.

We notice that both shell-model values are systematically smaller than those obtained within the density-function theory (see last column).

It will be interesting to see which of these results yield better agreement with CVC. However, now that the half-lives, branching ratios, and Q values are known with sufficient precision, measurements have to be carried out to determine the Fermi/Gamow-Teller mixing ratio ρ. With this goal, a letter of intent [38] has been submitted for the DESIR facility [39] at GANIL to determine the ρ parameter for ^{23}Mg.

6 Conclusions

Half-lives and branching ratios have been measured very precisely for the mirror β decays of ^{23}Mg and ^{27}Si. The half-life of ^{23}Mg has been determined with a precision of 0.03%. This value is in agreement with the latest measurements [14,15,16,17] but not with the two oldest values [12, 13]. If we exclude values with an uncertainty larger by a factor of 10 than the most precise value, the new average is 11.3053(44) s. Concerning the branching ratio of the super-allowed transition, the value presented in this work results in an uncertainty on the average value which is smaller by a factor of two from the previous error. The new average is 92.08(14)%, which represents a 0.15% precision.

Concerning the nucleus ^{27}Si, the half-life has been determined with a 0.05% precision. This value is in agreement with the previous average [3], but is about 8 times more precise. Adding this value to the others leads to a new average value of 4.1181(83) s which is twice more precise than the previous one. As for the branching ratio, the precision has not been improved, the average when adding our value remains the same as the previous one, i.e. 99.74(2)% (a 0.02% precision).

Finally, we propose new model calculations of the δ_c correction for the two nuclei of interest, which exploits a numbers of new ingredients with respect to Ref. [3]. To determine $\mathcal{F}t_0$ and V_{ud} an effort has to be made for the determination of the mixing parameter of Fermi and Gamow-Teller transitions, ρ.

Acknowlegdment

The authors would like to acknowledge the continuous effort of the whole Jyväskylä accelerator laboratory staff for ensuring a smooth running of the experiment. This work was supported by the Academy of Finland under the Finnish Centre of Excellence Programme 2012-2017 (Project No. 213503, Nuclear and Accelerator-Based Physics Research at JYFL), by the Conseil Régional d'Aquitaine, and by the European Community FP7 - Capacities - Integrated Infrastructure Initiative - contract ENSAR n^0 262010, and by the CFT (IN2P3/CNRS, France), AP théorie 2016.

References

1. J. C. Hardy and I. S. Towner, Phys. Rev. C **91**, 025501 (2015).
2. O. Naviliat-Cuncic and N. Severijns, Phys. Rev. Lett. **102**, 142302 (2009).
3. N. Severijns, M. Tandecki, T. Phalet, and I. S. Towner, Phys. Rev. C **78**, 055501 (2008).
4. C. Patrignani and Particle Data Group, Chin. Phys. C **40**, 100001 (2016).
5. I. D. Moore *et al.*, Nucl. Instr. Meth. B **317**, 208 (2013).
6. I. D. Moore, P. Dendooven, and J. Ärje, Hyp. Int. **223**, 17 (2014).
7. J. C. Hardy and I. S. Towner, Ann. Phys. (Berlin) **525**, 443 (2013).
8. O. Naviliat-Cuncic and N. Severijns, Eur. Phys. J. A **42**, 327 (2009).
9. B. Blank *et al.*, Nucl. Instr. Meth. A **776**, 34 (2014).
10. R. B. Firestone, Nucl. Dat. Sheets **108**, 1 (2007).
11. M. S. Basunia, Nucl. Dat. Sheets **112**, 1875 (2011).
12. M. V. Mihailovic and B. Povh, Nucl. Phys. **7**, 296 (1958).
13. J. D. Goss, F. L. Riffle, D. R. Parsignault, and J. C. Harris, Nucl. Phys. **A115**, 113 (1968).
14. D. E. Alburger, Phys. Rev. C **9**, 991 (1974).

15. G. Azuelos, J. Crawford, and J. E. Kitching, Nucl. Instr. Meth. **117**, 233 (1974).
16. G. Azuelos and J. E. Kitching, Phys. Rev. C **12**, 563 (1975).
17. G. Azuelos, J. E. Kitching, and K. Ramavataram, Phys. Rev. C **15**, 1847 (1977).
18. D. C. Sutton, PhD thesis, Princeton University (1962).
19. J. Black and J. Mahieux, Nucl. Instr. and Meth. **58**, 93 (1968).
20. D. Grober and W. Gruhle, BMBW-FBK **71-09**, 90 (1971).
21. H. Genz *et al.*, Nucl. Instr. and Meth. **134**, 309 (1976).
22. P. H. Barker, Nucl. Phys. **A275**, 37 (1977).
23. J. D. R. Talbert and M. G. Stewart, Phys. Rev. **119**, 272 (1960).
24. S. Gorodetzky, E. Aslanides, A. Gallmann, and G. Frick, Nucl. Phys. **A109**, 417 (1968).
25. F. Mann and R. Kavanagh, Nucl. Phys. A **235**, 299 (1974).
26. S. Gorodetzky *et al.*, Compt. Rend. Congr. Intern. Phys. Nucl., ed. Centre National de la Recherche Scientifique **vol. II**, 408 (1964).
27. D. F. H. S. D. Berenyi, D. A. Hutcheon and J. J. Weaver, Nucl. Phys. **A178**, 76 (1971).
28. C. Détraz, C. E. Moss, and C. S. Zaidins, Phys. Lett. **B34**, 128 (1971).
29. G. F. Grinyer, C. E. Svensson, and B. A. Brown, Nucl. Instr. Meth. A **622**, 236 (2010).
30. W. Satula, J. Dobaczewski, W. Nazarewicz, and T. R. Werner, Phys. Rev. C **86**, 054316 (2012).
31. I. S. Towner and J. C. Hardy, Phys. Rev. C **82**, 065501 (2010).
32. W. E. Ormand and B. A. Brown, Phys. Rev. Lett. **62**, 866 (1989).
33. B. A. Brown and W. D. M. Rae, Nucl. Data Sheets **120**, 115 (2014).
34. B. H. Wildenthal, Prog. Part. Nucl. Phys. **11**, 5 (1984).
35. B. A. Brown and W. A. Richter, Phys. Rev. C **74**, 034315 (2006).
36. W. E. Ormand and B. A. Brown, Nuc. Phys. **A491**, 1 (1989).
37. L. Xayavong, PhD thesis, University of Bordeaux, 2016 (unpublished).
38. P. Delahaye, private communication .
39. www.cenbg.in2p3.fr/desir .